

A map-based model predictive control approach for train operation

Michael Hauck, Patrick Schmidt, Alexander Kobelski, Stefan Streif

Abstract—Trains are a corner stone of public transport and play an important role in daily life. A challenging task in train operation is to avoid skidding and sliding, i.e. spinning or blocking of the wheels, during fast changes of traction conditions, which can, for example, occur due to changing weather conditions, crossings, tunnels or forest entries. The latter depends on local track conditions and can be recorded in a map together with other location-dependent information like speed limits and inclination. In this paper, a model predictive control (MPC) approach is developed. Thanks to the knowledge of future changes of traction conditions, the approach is able to avoid short-term skidding and sliding even under fast changes of traction conditions. In a first step, an optimal reference trajectory is determined by a multiple-shooting approach. In a second step, the reference trajectory is tracked by an MPC setup. The developed method is simulated along a track with fast-changing traction conditions for different scenarios, like changing weather conditions and unexpected delays. In all cases, skidding and sliding is avoided.

I. INTRODUCTION

A key aspect in train operation is slip control, since high slip results in flattened wheels and track damage. As a result, it decreases the reliability of train operation [1].

There exist a variety of approaches for anti-skid and anti-slip control. The majority of existing methods focus on re-adhesion control to decrease the slip after the start of skidding or sliding. For example, a re-adhesion control for a single-inverter multiple-induction-motors train system is presented in [2]. In order to suppress undesired slipping, the motor torque is controlled. In [3], a sliding-mode observer is developed to estimate the actual traction condition, which is used as an input for a second-order sliding-mode slip control. In [4], a re-adhesion slip control based on excessive torque and excessive angular momentum is presented. However, all re-adhesion slip control approaches have the disadvantage that they react after the occurrence of undesired slipping and thus, damage of wheels and track can not be avoided.

The emergence of undesired slipping can be tackled by active control approaches. In contrast to the re-adhesion or so-called "passive" slip controls, active slip controls [1], [5], [6] try to track the optimal adhesion value in order to avoid undesired slipping. The adhesion value is determined under the assumption that it depends only on slip. However, the

influence of weather and track conditions on the adhesion is neglected or at least reduced to two possible values, which may lead to unsafe scenarios [7]. For this reason, time-varying adhesion dynamics are introduced to tackle the changing traction conditions between wheel and track. A spatial iterative learning control is implemented to track the maximum adhesion. However, the maximum adhesion controls lead to severe impact and reduces the riding comfort [1].

Another possibility to avoid undesired slipping is to use model predictive control (MPC) approaches. MPC is a well-known method to solve optimal control problems. Both, input and state constraints can be incorporated easily via this method. In addition, updated data can be included to handle disturbances. Predictive control algorithms in train-motion control have been previously explored for various scenarios. For example, in [8], fuzzy predictive control is considered and the authors show in simulations that the performance of train safety, comfort, and other performance indicators are improved in comparison with conventional control technology. In [9], a predictive field-oriented control of the induction motor is developed based on estimation of the actual traction coefficient and measurement of actual wheel slip. A predictive speed profile tracking algorithm under linear constraints and under the assumption that the traction coefficient is constant is developed in [10]. Furthermore, in [11], an energy-efficient predictive train-motion control is developed, again, under the assumption of constant traction conditions. There, an optimal control problem is solved backwards in time via dynamic programming, which improves the driving mode by saving up to 40% of the consumed energy.

To the best of the authors' knowledge, existing predictive slip controls assume constant traction conditions over the prediction horizon. As a result, they fail to avoid skidding and sliding during fast changes of the traction conditions, which can, for example, occur during the entry in forests, tunnels or stations. In comparison to existing approaches in [10], [11], the current framework considers a variable traction coefficient, which is stored in a track-condition map together with topography data. Based on the knowledge of the future traction, a model predictive control approach is presented in this paper, which is able to avoid skidding and sliding even for fast changes in the traction conditions. Recording traction information and using it for vehicle operation has already been successfully applied in other scenarios, see [12], [13], [14], [15].

The rest of the paper is organized as follows: In Section II, the train-motion model and acceleration constraints are introduced. Additionally, the track-condition-and-topography

The authors are with Technische Universität Chemnitz, 09126 Chemnitz, Germany, Automatic Control and System Dynamics Lab (e-mail: {michael.hauck, patrick.schmidt, alexander.kobelski, stefan.streif}@etit.tu-chemnitz.de)

This research was funded by the German Ministry for Education and Research (BMBF) in the frame of the SRCC. EETCM project, grant number 03WIR1208.

©2023 the authors. This work has been accepted at the ECC for publication under a Creative Commons Licence CC-BY-NC-ND.

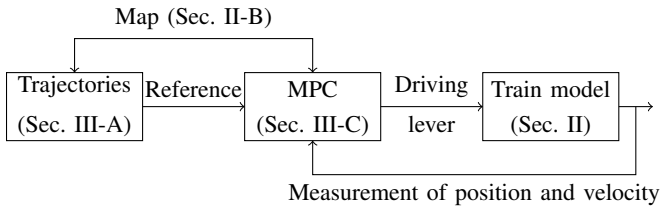


Fig. 1: Flow-chart of proposed map-based model predictive control approach for train operation.

map is presented as well as the optimal control problem. In Section III, a two-step solution approach is developed to solve the given problem. Section IV provides a case-study along with a discussion, where different situations like change of weather and unexpected delays are considered. Finally, the paper is concluded in Section V, presenting an outlook on further research topics. The whole setup is shown in Fig. 1.

Notation: The set of component-wise non-negative vectors in \mathbb{R}^n is defined as

$$\mathbb{R}_+^n := \{z = (z_1 \ \dots \ z_n)^\top \in \mathbb{R}^n : z_i \geq 0, \forall i = 1, \dots, n\}$$

for $n \in \mathbb{N}$. The set of piece-wise continuous functions mapping $[0, T]$ to \mathbb{R}_+ is denoted by $\mathcal{PC}^0([0, T], \mathbb{R}_+)$, similar for $\mathcal{C}^k([0, T], \mathbb{R}_+)$ as the set of k times continuously differentiable functions, where $k \geq 0$.

II. PROBLEM SETTING

In this section, a control-oriented model of the train dynamics and restrictions of the train motion are introduced. Afterwards, the concept of the track-condition-and-topography map, its content and how it is obtained is explained. In the end, the optimal control problem is stated.

A. Train dynamics

The train motion can be determined by a balance of force equation [16]:

$$ma = -F_r(v) + F_{\text{train}}(v)u, \quad (1)$$

where m is the train mass, a is the acceleration, v is the velocity, and u is the driving-lever position of the train. By convention, the latter is scaled in $[-1, 1]$; a positive value results in acceleration, a negative one in braking.

The resistance force in dependence of velocity v is given as [17]

$$F_r(v) = 1/2\rho_{\text{air}}c_{\text{air}}A_{\text{train}}(v-v_W)^2 + mg\sin(\alpha) + c_Rmg \quad (2)$$

and includes air resistance, inclination resistance, and rolling-resistance with ρ_{air} as air resistance coefficient, c_{air} as air density, A_{train} as effective area for train air resistance, v_W as wind speed in driving direction, g as gravitational constant, α as inclination, and c_R as rolling resistance coefficient.

The driving power $F_{\text{train}}(v)$ is a train-specific function, depending on the maximum train power and an internal limitation for small velocities [18]. Additionally, the driving power is limited by the maximum adhesion, which is addressed later by the introduction of train movement

restrictions. In [19] and [20], the driving power is shown for different trains and it can be approximated by

$$F_{\text{train}}(v) = k_1e^{-k_2v} + k_3,$$

where the coefficients $k_i > 0$ can be determined by a least-squares approach for a specific train.

Let p be the position of the train and define $x = (p \ v)^\top$. Thus, the train-motion model can be written as the following input-affine state-space model:

$$\dot{x} = \underbrace{\begin{pmatrix} x_2 \\ -\frac{F_r(x_2)}{m} \end{pmatrix}}_{=:f(x;m)} + \underbrace{\begin{pmatrix} 0 \\ \frac{k_1e^{k_2x_2} + k_3}{m} \end{pmatrix}}_{=:g(x;m)} u. \quad (3)$$

By $f_i(x; m)$, the i -th component of $f(x; m)$ is denoted. Train motion further depends on local track conditions and the topography of the track, which are summarized in a track-condition-and-topography map. Such a map is described in the next section.

B. Track-condition-and-topography map

Usually, trains travel along the same routes with location-dependent speed limits, inclination, weather-dependent traction parameters etc. If skidding or sliding occurs due to location-dependent reasons at a certain point, it can be assumed that this will happen again on the next trip. By recording such information in a track-condition-and-topography map, subsequent train rides can exploit this information to improve their performance, e.g. avoiding high slip by preemptively throttling down the engine torque. For ease of notation, the track-condition-and-topography map is denoted as map from now on.

In this paper, we assume a standard passenger train on a commercially operated line with multiple stops. The train must follow a timetable and adhere to speed limits. The track follows the topography of the terrain, so the train ride is affected by the inclination. Furthermore, the traction conditions of the rails are subject to environmental influences.

For this work we assume a setup, where the map contains:

- inclination at position p : $\alpha(p)$,
- maximal velocity limit at position p : $v_{\text{max}}(p)$,
- two exemplary traction trajectories for maximal traction (also known as maximum adhesion coefficient) at position p : $\mu_j(p)$ $j \in \{\text{good}, \text{bad}\}$ (based on environmental conditions), and
- time table including arrival time t_{station_i} at station p_{station_i}

Two different μ -trajectories will be used in the case study, to show performance on good as well as bad track conditions. Based on this information, a map is created, see Fig. 2. Bad conditions may refer to track conditions in freezing weather or as soon as rain begins to fall, when water mixes with dust to a muddy film on the tracks. Note, that for future references of μ , the maximum value for the given track conditions ('good' or 'bad') is denoted by μ_{max} .

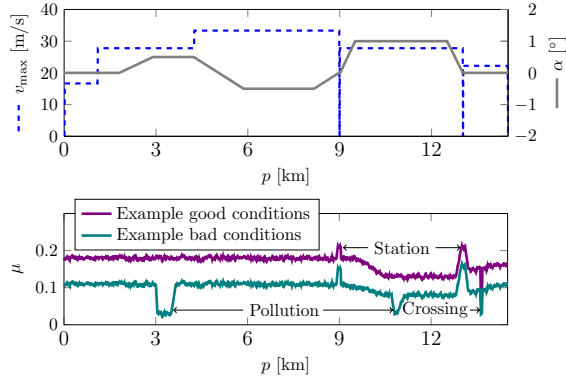


Fig. 2: Map used in case study in Section IV. Velocity limits, inclination and time table are based on train ride from RB30 Chemnitz to Cranzahl, Germany. Traction trajectories were built based on measurements from [13].

C. Constraints

Train motion is restricted due to physical limitations (traction, engine, and brakes) as well as safety of passengers. The acceleration is limited by the following restrictions: (i) safety restrictions for the passengers during braking and acceleration

$$|f_2(x; m) + g_2(x; m)u| \leq a_{\max}, \quad (4)$$

with $a_{\max} > 0$ and (ii) the maximum traction at the current position p

$$|g_2(x; m)u| \leq \mu_{\max}(x_1)g. \quad (5)$$

The maximum traction μ_{\max} depends on the position and is defined in the next section. Furthermore, acceleration is restricted by the maximum engine power and braking force. Both are already included in the model description with the assumption, that a driving lever position takes value between 1 and -1 , where $u = 1$ yields maximum engine power and $u = -1$ maximum braking force.

The total mass of the train m is the mass of its own weight m_{train} plus the load given by passengers and luggage, where the maximal additional load is defined as m_{maxload} . Thus, the following inequality holds for the mass of the train:

$$m_{\min} := m_{\text{train}} \leq m \leq m_{\text{train}} + m_{\text{maxload}} =: m_{\max}. \quad (6)$$

The mass of the train varies due to a changing number of passengers and luggage. It is constant between two stations, but unknown in most cases. Therefore, the constraints (4) and (5) have to be satisfied for all $m \in [m_{\min}, m_{\max}]$. Depending on whether the train is braking or accelerating, either the minimum mass or the maximum mass yields the highest value in (4) and (5). Therefore, these masses are inserted into the respective inequalities. Inequality constraints on both, states and control are incorporated via the function

$h : \mathbb{R}^2 \times [-1, 1] \rightarrow \mathbb{R}^7$ with

$$h(x, u) = \begin{pmatrix} f_2(x; m_{\min}) + g_2(x; m_{\min})u - a_{\max} \\ -(f_2(x; m_{\max}) + g_2(x; m_{\max})u) - a_{\max} \\ g_2(x; m_{\min})u - \mu_{\max}(x_1)g \\ -g_2(x; m_{\max})u - \mu_{\max}(x_1)g \\ x_2 - v_{\max}(x_1) \\ -1 - u \\ u - 1 \end{pmatrix}. \quad (7)$$

D. Optimal control problem

Along with train-motion dynamics (1), an optimal control problem is formulated. The solution to the optimal control problem yields the desired lever position as a control input for the model and is defined as:

$$\begin{aligned} u^* &= \arg \min_{u \in \mathbb{U}} \frac{1}{2} \int_{t_0}^{t_{\text{station}}} u^2 dt \\ \text{s.t. } \dot{x} &= f(x; m) + g(x; m)u, \\ x(t_0) &= x_0, x(t_{\text{station}}) \in \mathcal{X}_{\text{station}}, \\ h(x, u) &\leq 0. \end{aligned} \quad (8)$$

The objective function is chosen to minimize the norm of the input within the time interval $[t_0, t_{\text{station}}]$, where t_{station} is the desired arrival time at the station provided by the map. As a solution to the optimal problem, a continuous function $u^* \in \mathbb{U} := \mathcal{C}^0([t_0, t_{\text{station}}], [-1, 1])$ is obtained. It is assumed that a feasible solution exists for all station with initial condition $x_0 \in \{p_0\} \times [0, v_{\max}(p_0)]$, where $v_{\max}(p_0)$ is the speed limit at $p_0 \in \mathbb{R}_+$. As a terminal condition at $t = t_{\text{station}}$, the train has to stop at the station given at p_{station} . This terminal condition is replaced by a relaxed one, which is given by $\mathcal{X}_{\text{station}}$ increasing the amount of feasible solutions. The tolerance for the terminal position is given as $\varepsilon_1 \geq 0$. Therefore, the terminal set is given as $\mathcal{X}_{\text{station}} := [p_{\text{station}} - \varepsilon_1, p_{\text{station}} + \varepsilon_1] \times \{0\}$.

III. METHODS

Since the computation of u^* in (8) is associated with high computing time, the optimal control problem has to be adjusted in order to decrease the computation burden in view of applicability. To this end, a two-step approach is considered. In the first step, u^* as defined in (8) is computed to obtain a reference trajectory $u_{\text{ref}}^c := u^*$ for all $t \in [t_0, t_{\text{station}}]$. Then, u^* is applied to system (1) to obtain the reference trajectory $x_{\text{ref}}^c \in \mathcal{C}^1([t_0, t_{\text{station}}], \mathbb{R}_+^2)$. In a second step, these trajectories are tracked online via MPC.

A. Computation of reference trajectories

The reference trajectory for the input u is defined via (8) and it is computed with a multiple-shooting method, which is a powerful solution approach to tackle boundary value problems [21]. In multiple-shooting methods, the interval $[t_0, t_{\text{station}}]$ is divided into $m_\ell - 1$ subintervals denoted as $[t_i, t_{i+1}]$, $i = 1, 2, \dots, m_\ell - 1$, where m_ℓ is given as the

number of nodes, $t_1 := t_0$, and $t_{m_\ell} := t_{\text{station}}$. On each of the subintervals, the given problem is solved for initial values $x(t_i)$. In further steps, the initial values are adjusted such that the states at the end of $[t_i, t_{i+1}]$ coincide with the initial value of the next subinterval, i.e. $x(t_{i+1})$. At the end, the boundary condition at the right-hand side of $[t_i, t_{i+1}]$ and the initial condition of $[t_{i+1}, t_{i+2}]$ are the same for $i = 1, 2, \dots, m_\ell - 2$, which yields the desired solution $u_{\text{ref}}^c \in \mathcal{PC}^0([t_0, t_{\text{station}}], [-1, 1])$.

Once u_{ref}^c is computed, it is applied to system (1) to obtain the reference trajectory $x_{\text{ref}}^c \in \mathcal{C}^1([t_0, t_{\text{station}}], \mathbb{R}_+^2)$, which are tracked in the second step of the procedure, namely the model predictive control. Since these trajectories provide a feasible solution, the prediction horizon can be reduced in order to decrease the computation time, since minimizing the distance to the trajectory ensures the satisfaction of the terminal condition. To decrease the computational burden of the tracking MPC, the system dynamics (3) are first linearized at the reference trajectories x_{ref}^c and u_{ref}^c . Afterwards, the linearized model is discretized for the implementation.

B. Linearization and discretization

Using Taylor approximation, the linearized model with states $x_{\text{lin}} := x - x_{\text{ref}}^c$ and control $u_{\text{lin}} := u - u_{\text{ref}}^c$ reads as

$$\dot{x}_{\text{lin}} = \underbrace{\begin{pmatrix} 0 & 1 \\ a_{21}(t) & a_{22}(t) \end{pmatrix}}_{=A_{\text{lin}}(t)} x_{\text{lin}} + \underbrace{\begin{pmatrix} 0 \\ b_2(t) \end{pmatrix}}_{=b_{\text{lin}}(t)} u_{\text{lin}}. \quad (9)$$

The remaining entries are calculated as

$$a_{21}(t) = \frac{\partial f_2(x; m)}{\partial \alpha} \frac{\partial \alpha}{\partial x_1} = -g \cos(\alpha_{\text{ref}}(t)) \frac{d\alpha}{dx_1}$$

with $\alpha_{\text{ref}}(t)$ as inclination at $x_{\text{ref}_1}^c(t)$ and $\frac{\partial \alpha}{\partial x_1}$ given from the map, as well as

$$a_{22}(t) = -\frac{1}{m} \varrho_{\text{air}} c_{\text{air}} A_{\text{train}} (x_{\text{ref}_2}^c(t) - v_W) - \frac{1}{m} k_1 k_2 e^{-k_2 x_{\text{ref}_2}^c(t)} u_{\text{ref}}^c(t)$$

and

$$b_2(t) = \frac{k_1 e^{-k_2 x_{\text{ref}_2}^c(t)} + k_3}{m}.$$

After linearizing the train-motion dynamics (1), the obtained model (9) is discretized. The sampled states are defined as

$$x_{\text{ref}_i}^d = (x_{\text{ref}_i}^c(t_{\text{step}}) \quad x_{\text{ref}_i}^c(2t_{\text{step}}) \quad x_{\text{ref}_i}^c(3t_{\text{step}}) \quad \dots)^\top$$

for $i = 1, 2$, where x_{ref}^d is defined analogously.

The resulting discrete-time model is given by

$$x^d(k+1) = A^d(k)x^d(k) + b^d(k)u^d(k), \quad (10)$$

where

$$A^d(k) = e^{A_{\text{lin}}(kt_{\text{step}}) \cdot t_{\text{step}}}$$

and

$$b^d(k) = \int_0^{t_{\text{step}}} e^{A_{\text{lin}}(kt_{\text{step}}) \cdot (t_{\text{step}} - \tau)} b_{\text{lin}}(kt_{\text{step}}) d\tau.$$

C. Tracking MPC

The linearized and discretized model is used in the optimal control problem along with the reference trajectories from Section III-B. An MPC setup with moving horizon N is considered to track $x_{\text{ref}_1}^d$, which results in minimizing the difference between the current position at $t = kt_{\text{step}}$ and $x_{\text{ref}_1}^d(k)$. This difference is defined as $x_1^d(k)$ in (10). In order to increase the amount of feasible solutions, the terminal constraint in (8) is replaced by terminal costs. Therefore, the cost function of the optimal control problem (8) is enlarged by terminal costs to obtain the resulting tracking MPC as

$$\begin{aligned} \min_U \quad & \frac{1}{2} U^\top R U + \frac{1}{2} X_1^\top Q X_1 \\ \text{s.t.} \quad & x^d(k+1) = A^d(k)x^d(k) + b^d(k)u^d(k), x^d(0) = x_0, \\ & h(x^d(k), u^d(k)) \leq 0 \quad \forall k = j, \dots, j+N-1. \end{aligned} \quad (11)$$

In the objective function, $U, X_1 \in \mathbb{R}^N$ are weighted via $R, Q \in \mathbb{R}^{N \times N}$, $R, Q \succ 0$. At time instant j , $X_1 = (x_1^d(j) \quad \dots \quad x_1^d(j+N-1))^\top$ includes $x_{\text{ref}_1}^d(j), \dots, x_{\text{ref}_1}^d(j+N-1)$ as reference trajectory values. Analogously, the input vector is defined as $U = (u^d(j) \quad \dots \quad u^d(j+N-1))^\top$.

The solution of (11) is denoted as U^* . Once the optimal control sequence is obtained, only the first element of U^* is applied to the system (1), which yields a new initial value for the next iteration. Afterwards, the horizon is shifted and, in particular, the reference values in X_1 are updated. This iterative scheme is applied until the arrival station is reached. Note that if the remaining prediction length is smaller than N , then N is reduced to the remaining length.

IV. IMPLEMENTATION AND CASE-STUDY

In this section, the proposed multiple-shooting method and the tracking MPC are implemented and simulated for the RB30, traveling from Chemnitz to Cranzahl, Germany. Physical parameters of the train, as well as the used tuning parameters of the multiple-shooting approach and the tracking MPC are listed. With these parameters, three different scenarios (e.g. behavior for good traction conditions, weather change, and delays) are simulated and analyzed.

A. Parameters

For the simulations presented in this section, the train-specific model parameters and physical constants shown in Table I are used. They result from train data sheets, whereas k_i are determined by a least-squares approach.

TABLE I: Train-specific model parameter.

Parameter	Value
ϱ_{air}	1.2041 kg/m ³
A_{train}	10 m ²
c_{air}	0.85
c_{r}	0.002
k_1	1.516×10^5 kgm/s ²
k_2	0.1147 1/s
k_3	1.564×10^4 kgm/s ²
m_{train}	68 200 kg
m_{maxload}	20 500 kg

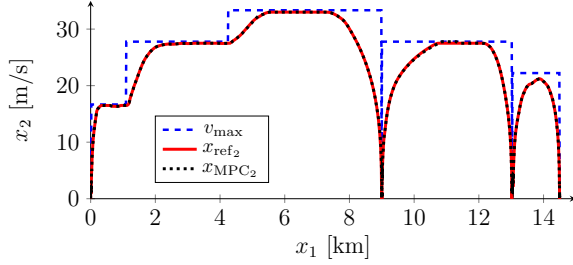


Fig. 3: Comparison of reference velocity according to multiple-shooting approach and the velocity determined by tracking MPC for the first three railway sections.

The train-track-specific parameters like the speed limit $v_{\max}(x_1)$, the inclination $\alpha(x_1)$, and the maximal traction $\mu_{\max}(x_1)$ are listed in the map (see Section II and Fig. 2). In the simulations, the wind speed in driving direction was assumed by $v_w = 0$.

For the implementation of the multiple-shooting method, the number of subintervals m_ℓ is determined depending on t_{station} , such that the time between two subintervals is less than three seconds, i.e. $m_\ell = \lfloor t_{\text{station}}/3 \rfloor$. In the simulations it turned out to be a good trade-off between accuracy and computational effort. However, the number of subintervals can be increased, since the computation is done offline. For the implementation of the MPC setup, the discretization time $t_{\text{step}} = 1$ second and the horizon length $N = 20$ are used. The mass of the train $m = 78200\text{kg}$ is determined as the sum of the empty train mass and an average passenger weight value. The weighting matrices are chosen as $R = 0.01I_N$ and $Q = I_N$, where I_N is the $N \times N$ identity matrix. These values are tuned manually, such that tracking of optimal states x and the optimal input u is fulfilled in all considered simulations.

B. Simulation results

In a first scenario, the behavior of the train is simulated and analyzed for good traction conditions. Afterwards, a change in the traction conditions due to fallen leaves or frozen railway resulting in a different $\mu_{\max}(x_1)$ is analyzed. In a third simulation, the effects of an unplanned delay are investigated.

In Fig. 3, the reference velocity according to multiple-shooting approach as well as the resulting velocity determined by tracking MPC is shown. The difference between them is shown in Fig. 4 together with the resulting tracking error between the reference trajectory x_{ref_1} and the train position x_1 according to tracking MPC is shown in Fig. 4. The tracking MPC approach is able to track the reference with a maximal position error of around 5 m and a maximal velocity error of less than 3 m/s.

Furthermore, the satisfaction of the constraints (7) is considered. The first two elements $h_1(x, u)$ and $h_2(x, u)$ describe the safety constraints, whereas $h_3(x, u)$ and $h_4(x, u)$ describe maximum traction. In Fig. 5, the maximum of the safety constraints as well as the traction constraints are visualized. It can be seen that the safety constraints are more

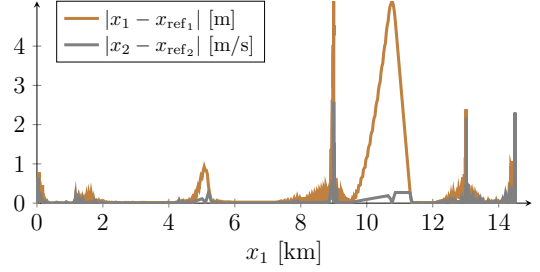


Fig. 4: Resulting tracking error between the reference trajectory x_{ref} and the calculated states x according to tracking MPC for good traction conditions.

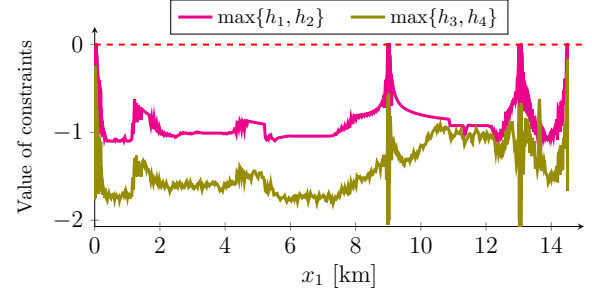


Fig. 5: Safety and traction constraints of tracking MPC with good traction conditions.

restrictive than traction constraints. However, all constraints are satisfied since all $h_i(x, u) \leq 0$ along the whole track.

In a next step, the influence of changing traction conditions between two stations is analyzed. There exist two possible cases, namely that the new traction conditions are better or worse than the assumed ones. The first case is not problematic, since the bad weather reference trajectory can be easily tracked with better traction conditions. In the other case, a decrease of the maximal traction yields a decrease of maximal acceleration and braking.

For this scenario, the reference trajectories for good traction conditions are tracked via MPC. However, due to an unexpected change of the weather conditions, the traction is changing to bad conditions immediately after leaving the station (cf. traction trajectories in the map in Fig. 2). The tracking error yields no significant change. More interesting is, that the traction constraints are more restrictive at the bigger part of the track, which can be seen in Fig. 6. However, the constraints are satisfied along the whole track. Therefore, the developed approach is able to avoid skidding and sliding during changes of weather conditions.

In a third scenario, the effects of an unexpected delay due to longer passenger changing time are analyzed. An initial delay of $t_{\text{delay}} = 40$ seconds in the first station was simulated under good traction conditions. With this delay, the optimal control problem (8) is infeasible, since the train can not reach the first station in the given time. However, the reference trajectories are calculated offline independently of the occurred delay, thus, they are feasible for the initial time table. Since terminal constraints are replaced by terminal costs in the MPC approach, the OCP (11) obtains a feasible

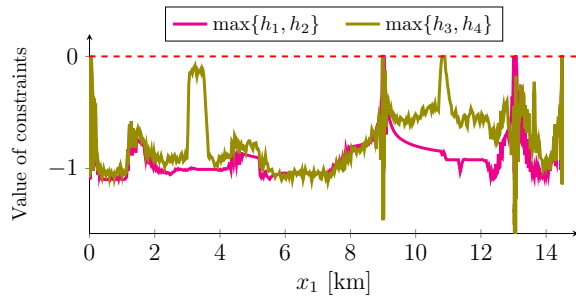


Fig. 6: Safety and traction constraints of tracking MPC with bad traction conditions.

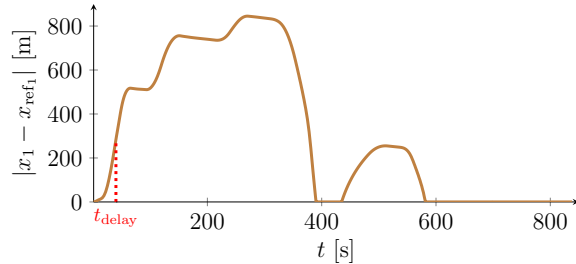


Fig. 7: Tracking error with an initial delay of 40 seconds.

solution. As shown in Fig. 7, the tracking error caused by the delay at position $x_1(t_{\text{delay}}) = 0$ is around 280 meters. The train arrives at the next station with a delay of 19 seconds, which is smaller than the initial one. Due to waiting time in the station, the tracking error is zero for a short moment until the desired departure. Until the following station, the tracking error decreases to zero and the MPC tracks the reference from this point on. Again, all constraints are satisfied at each point. Therefore, especially skidding and sliding is prevented.

V. CONCLUSION AND OUTLOOK

This paper proposes a model predictive control approach for train operation. The presented approach is able to avoid skidding and sliding during fast changes of the traction conditions, by using a map with traction conditions and topography data. In order to reduce the computational effort in online operation, the optimal control problem is solved offline to generate reference trajectories for the position, velocity and the lever position. Afterwards, a tracking MPC setup follows the reference trajectories.

In a case-study, it turned out that the MPC tracks the reference trajectory with a small tracking error while satisfying all constraints. Furthermore, even with changing weather conditions, MPC yields a feasible solution, where traction conditions became more restrictive in this case. Additionally, the developed approach was able to handle unexpected delays.

In future works, a more detailed model can be considered including, for example, motor characteristics and different braking functions. Another future idea is an online adaption of the map based on actual measurements. Furthermore, information that are available shortly before they have to be considered are important extensions. Those ones include,

e.g., blocked sections by other trains or environmental influences.

REFERENCES

- [1] W.-C. Cai, D.-Y. Li, and Y.-D. Song, "A novel approach for active adhesion control of high-speed trains under antiskid constraints," *IEEE Transactions on Intelligent Transportation Systems*, vol. 16, no. 6, pp. 3213–3222, 2015.
- [2] Y. Matsumoto, N. Eguchi, and A. Kawamura, "Novel re-adhesion control for train traction system of the "Shinkansen" with the estimation of wheel-to-rail adhesive force," in *IECON'01. 27th Annual Conference of the IEEE Industrial Electronics Society (Cat. No. 37243)*, vol. 2. IEEE, 2001, pp. 1207–1212.
- [3] M. Amodeo, A. Ferrara, R. Terzaghi, and C. Vecchio, "Wheel slip control via second-order sliding-mode generation," *IEEE Transactions on Intelligent Transportation Systems*, vol. 11, no. 1, pp. 122–131, 2009.
- [4] T. Hara and T. Koseki, "Study on re-adhesion control by monitoring excessive angular momentum in electric railway tractions," in *2012 12th IEEE International Workshop on Advanced Motion Control (AMC)*. IEEE, 2012, pp. 1–6.
- [5] J.-S. Hu, D. Yin, Y. Hori, and F.-R. Hu, "Electric vehicle traction control: a new mtte methodology," *IEEE Industry Applications Magazine*, vol. 18, no. 2, pp. 23–31, 2011.
- [6] W. Liao, H. Chen, W. Cai, and Y. Song, "A novel active adhesion control design for high speed trains without vehicle speed measurement," in *Proceedings of the 33rd Chinese Control Conference*. IEEE, 2014, pp. 221–226.
- [7] D. Huang, W. Yang, T. Huang, N. Qin, Y. Chen, and Y. Tan, "Iterative learning operation control of high-speed trains with adhesion dynamics," *IEEE Transactions on Control Systems Technology*, vol. 29, no. 6, pp. 2598–2608, 2021.
- [8] Y. Cao, L. Ma, and Y. Zhang, "Application of fuzzy predictive control technology in automatic train operation," *Cluster Computing*, vol. 22, no. 6, pp. 14 135–14 144, 2019.
- [9] S. Sadr, D. A. Khaburi, and J. Rodríguez, "Predictive slip control for electrical trains," *IEEE Transactions on Industrial Electronics*, vol. 63, no. 6, pp. 3446–3457, 2016.
- [10] A. Molavi and F. Rashidi Fathabadi, "Robust model predictive anti-slip controller and speed profile tracking of an electric train based on lmi approach," *International Journal of Dynamics and Control*, pp. 1–12, 2022.
- [11] H. Novak, V. Lešić, and M. Vašak, "Energy-efficient model predictive train traction control with incorporated traction system efficiency," *IEEE Transactions on Intelligent Transportation Systems*, vol. 23, no. 6, pp. 5044–5055, 2021.
- [12] A. Kobelski, P. Osinenko, and S. Streif, "A method of online traction parameter identification and mapping," *IFAC-PapersOnLine*, vol. 53, no. 2, pp. 13 933–13 938, 2020.
- [13] K. Nagase, "A study of adhesion between the rails and running wheels on main lines: results of investigations by slipping adhesion test bogie," *Proceedings of the Institution of Mechanical Engineers, Part F: Journal of Rail and Rapid Transit*, vol. 203, no. 1, pp. 33–43, 1989.
- [14] P. Osinenko, M. Geißler, and T. Herlitzius, "Adaptive unscented kalman filter with a fuzzy supervisor for electrified drive train tractors," in *2014 IEEE International Conference on Fuzzy Systems*. IEEE, 2014, pp. 322–331.
- [15] P. Osinenko, M. Geißler, T. Herlitzius, and S. Streif, "Experimental results of slip control with a fuzzy-logic-assisted unscented kalman filter for state estimation," in *2016 IEEE International Conference on Fuzzy Systems*. IEEE, 2016, pp. 501–507.
- [16] X. Yao, J. H. Park, H. Dong, L. Guo, and X. Lin, "Robust adaptive nonsingular terminal sliding mode control for automatic train operation," *IEEE Transactions on Systems, Man, and Cybernetics: Systems*, vol. 49, no. 12, pp. 2406–2415, 2018.
- [17] D. Wende, *Fahrdynamik des Schienenverkehrs*. Springer-Verlag, 2013.
- [18] J. Ihme, *Schienefahrzeugtechnik*. Springer, 2016.
- [19] A. Steimel, *Electric traction: motive power and energy supply*. Division Deutscher Industrieverlag, 2014.
- [20] J. Golling. (2020) Bahntechnik & bahnbetrieb. [Online]. Available: <https://www.bahntechnik-bahnbetrieb.de/beschleunigungsrechner/>
- [21] R. Bulirsch, J. Stoer, and J. Stoer, *Introduction to numerical analysis*. Springer, 2002, vol. 3.